J. Min. Metall. Sect. B-Metall. 55 (2) B (2019) 157 - 166

Journal of Mining and Metallurgy, Section B: Metallurgy

EXPERIMENTAL INVESTIGATION AND THERMODYNAMIC CALCULATIONS OF THE Bi-Ni-Pb PHASE DIAGRAM

D. Minić [a,*], M. Premović [a], N. Tošković [b], D. Manasijević [c], V. Ćosović [d], M. Janaćković [a], M. Tomović [a]

[a] University in Priština, Faculty of Technical Sciences, Kos. Mitrovica, Serbia
[b] University of East Sarajevo, Faculty of Technology, Zvornik, Bosnia and Herzegovina
[c] University of Belgrade, Technical Faculty, Bor, Serbia
[d] University of Belgrade, Institute of Chemistry, Technology and Metallurgy, Belgrade, Serbia

(Received 28 November 2018; accepted 02 April 2019)

Abstract

The article presents an experimental study of a phase diagram of a ternary Bi-Ni-Pb system using differential thermal analysis (DTA), scanning electron microscopy (SEM) with energy dispersive spectrometry (EDS), and X-ray powder diffraction (XRD) analysis. The investigated ternary alloys were selected from three vertical sections (x(Bi)=0.75, x(Ni)=0.1 and x(Pb)=0.9) and two isothermal sections at 100 and at 300 °C. The obtained experimental results were compared with the thermodynamically extrapolated phase diagram of the Bi-Ni-Pb ternary system based on the thermodynamic parameters for the constitutive binary systems available in literature. Reasonably close agreement between the experimental data and the calculated phase diagram was obtained.

Keywords: *Bi–Ni-Pb system; Vertical sections x(Bi)=0.75, x(Ni)=0.1 and x(Pb)=0.9; Isothermal sections at 100 and at 300 °C; Thermal analysis; Thermodynamic prediction*

1. Introduction

It is well known that phase diagrams provide valuable information which can be really helpful to the industry in its search for the best and the most practical applicable alloys. Keeping that in mind, accurate and detailed description of phase diagrams is a rather important task for researchers. Generally, a good approach to assessing phase diagrams is by combining experimental results and thermodynamic predictions using Calphad method [1,2], since it provides a reliable description of total Gibbs energies of phases. Such described Gibbs energies of phases can be subsequently used for visualization of phase diagrams by means of software packages such as Pandat [3], ThermoCalc [4], OpenCalphad [5], and many others. Up to now, for most of the binary systems reliable thermodynamic datasets of total Gibbs energies of phases have been made available. Given that typically applicable alloys consist of more elements, it is, therefore, necessary to study systems which consist of three, four and more elements. Hence, the focus of presented study is on experimental investigation of phase equilibria in a ternary Bi-Ni-Pb system, especially since, to the extent of our knowledge, the ternary Bi-Ni-Pb system has not been experimentally investigated before. An additional motivation for this study was based on the technical importance of the Bi-Ni based systems [6-8]. According to the technical importance of the Bi-Ni based systems, possible application of the ternary Bi-Ni-Pb alloys is in the electronic devices and as a semiconductor.

In the course of the present study, three series of the samples (as-cast samples, samples annealed at 100 and at 300 °C) were prepared for experimental investigation. The as-cast samples from three vertical sections were investigated using differential thermal analysis (DTA). The samples annealed at 100 and 300 °C were studied by means of scanning electron microscopy (SEM) together with energy dispersive spectrometry (EDS) and X-ray diffraction analysis (XRD) with samples in a powder form.

In parallel with that, phase diagrams of the investigated ternary system Bi-Ni-Pb were calculated by using thermodynamic parameters for the constitutive binary systems reported in literature [9-13]. The calculated results that include phase diagrams of the experimentally investigated sections, liquidus projection, and invariant reactions were

**Corresponding author: dminic65@mts.rs*

DOI:10.2298/JMMB181128024M

CC BY SA

compared with the obtained experimental results, and a close mutual agreement was observed.

2. Experimental procedure

All studied ternary alloy samples were prepared from high purity (99.999 at. %) Bi, Ni and Pb elements, produced by Alfa Aesar (Germany). Individual masses of samples were about 3 g. The elements were used as received from the supplier. In total 23 samples were prepared. All ternary samples weighing, the corresponding sample mixtures with the chosen compositions, were melted in an induction furnace. Such prepared samples were divided into three groups. One group of 12 samples was used for DTA test. The alloy samples from second (5 samples) and third groups (6 samples) were intended for SEM-EDS and XRD investigation. Samples from second group were put into quartz glass ampoules, sealed under vacuum, and annealed at 100 °C. Samples from third group were put into quartz glass ampoules, sealed under vacuum, and annealed at 300 °C. After five and eight weeks of annealing, respectively, the samples were quenched into ice water in order to preserve the equilibrium compositions at the nominated temperatures.

For determination of chemical compositions of the samples and coexisting phases within their microstructures, JEOL JSM-6460 scanning electron microscope (SEM) with energy dispersive spectrometer (EDS) (Oxford Instruments X-act) was employed. The overall compositions of the annealed and quenched alloy samples were determined by analysis of the as large as possible surface of the samples. The compositions of the co-existing phases within the studied samples were determined by examining the surface of the same phase at different regions of the sample.

Phase identification of the alloy samples in a powder form were recorded on a XRD devices D2 PHASER (Bruker, Karlsruhe, Germany). Patterns were recorded in a 2θ range from 10° to 75° with a step size of 0.02°. The patterns were analyzed using the Topas 4.2 software, ICDD databases PDF2 (2013) [14].

Phase transition temperatures were determined by DTA method using Shimadzu DTG 60 H instrument, calibrated with high purity elements Ag, In, Zn produced by Alfa Aesar. The studied alloy samples were placed in alumina crucibles and the analysis was performed under flowing high purity argon 6.0 (99.9999 %) atmosphere supplied by MESSER. The sample mass of 30 mg and the heating rate of 5 °C/min with three cycles of heating and cooling were adopted for the conducted investigations. Three cycles were conducted in way to get more precise results. The temperatures determined in this study were taken from the second cycle, since determined temperatures of the second and third heating cycles were close to each other. The temperatures from the first cycle were omitted due to deviations from the temperatures recorded in the second and third cycles. The reference material in each case was an empty alumina crucible.

3. Thermodynamic calculation of binary systems

Constitutive binary sub systems of the ternary Bi-Ni-Pb system have been extensively studied in the past and reliable thermodynamic datasets for these binary systems are available. The binary end-systems (Bi–Ni, Bi–Pb, Ni–Pb) were reproduced in Fig. 1 in order to provide some general notions about their key features. The calculation of the phase diagrams was done using Pandat software [3] and corresponding literature data.

The binary Bi-Ni phase diagram was calculated with parameters optimized by Vassilev et al. [9-11] (Figure 1.a). The phase diagram of the Bi-Pb system was calculated using parameters reported by Boa and Ansara [12], (Figure 1.b). The binary Ni-Pb phase diagram was calculated by using thermodynamic parameters obtained by Wang et al. [13], (Figure 1.c).

Used thermodynamic parameters for calculation are summarized in Table 1.

The phases, which are according to the available literature information on the phase equilibria and the crystallographic data, are summarized in Table 2.

As can be seen in Table 2, liquid phase, four solid solution phases (Bi), (Ni), (Pb) and (εPb), and two binary intermetallic compounds Bi_3Ni and BiNi should appear in the investigated ternary system.

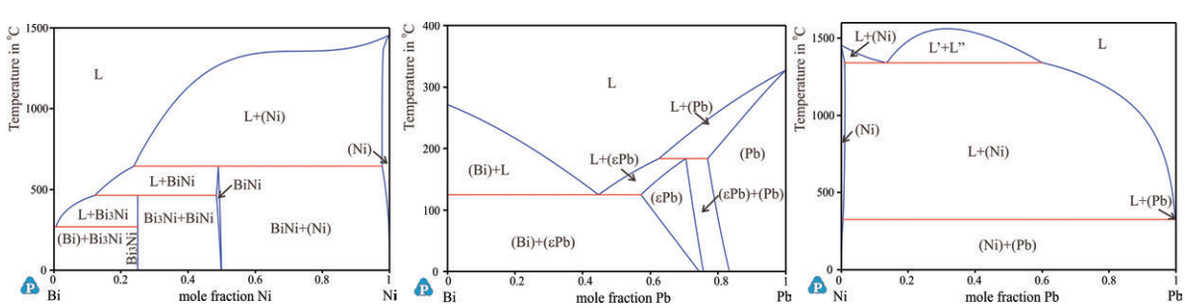

Figure 1. *Calculated phase diagrams a) binary Bi-Ni system, b) binary Bi-Pb system and c) binary Ni-Pb system*

CC BY SA

Table 1. *Thermodynamic parameters of the ternary Bi-Ni-Pb system [9-13]*

Phase and thermodynamic model	Thermodynamic parameters
$LIQUID(Bi,Ni,Pb)$	${}^{0}L^{Liquid}_{Bi,Ni} = -6440 + 13.288T$
	${}^{1}L^{Liquid}_{Bi,Ni} = -11315 - 1.457T$
	${}^{0}L^{Liquid}_{Ni,Pb} = 31532.257 - 2.425T$
	${}^{1}L^{Liquid}_{Ni,Pb} = 10459.949 - 2.498T$
	${}^{2}L^{Liquid}_{Ni,Pb} = -10927.180 + 7.952T$
	${}^{3}L^{Liquid}_{Ni,Pb} = -3732.467 - 0.109T$
	${}^{0}L^{Liquid}_{Bi,Pb} = -4330.3 - 2.0421T + 0.06542T\ln(T)$
	${}^{1}L^{Liquid}_{Bi,Pb} = 1.53 - 1.02298T$
	${}^{2}L^{Liquid}_{Bi,Pb} = 896.7 - 1.2644T$
$FCC\_A1(Bi,Ni,Pb)_1(Va)_1$	${}^{0}L^{Fcc\_A1}_{Bi,Ni:Va} = 5030 + 17T$
	${}^{0}L^{Fcc\_A1}_{Ni,Pb:Va} = 29980 + 0.59T$
	${}^{1}L^{Fcc\_A1}_{Ni,Pb:Va} = -20000 + 25T$
	${}^{0}L^{Fcc\_A1}_{Bi,Pb:Va} = -2852.75 - 3.5832T$
$HCP\_A3(Bi,Pb)_1(Va)_{.5}$	${}^{0}L^{Hcp\_A3}_{Bi,Pb:Va} = -4441.67 - 7.4411T$
	${}^{1}L^{Hcp\_A3}_{Bi,Pb:Va} = 1725.26 - 4.0220T$
$RHOMBO\_A7(Bi,Pb)$	${}^{0}L^{Rhombo\_A7}_{Bi,Pb} = 3461.59 + 45.2234T$
$BINI(Bi)_{.5}(Ni,Va)_{.5}$	${}^{0}L^{BiNi}_{Bi:Va} = -4983 + 15.252T - 2.0967E - 6T^3 + .5G^{Hex}_{Bi}$
	${}^{0}L^{BiNi}_{Bi:Ni} = -10392 + 5.001T - 3.558E - 7T^3 + .5G^{Hex}_{Bi} + .5G^{H}_{Ni}$
	${}^{0}L^{BiNi}_{Bi:Ni,Va} = 0$
$BI3NI(Bi)_{.75}(Ni)_{.25}$	${}^{0}L^{Bi_3Ni}_{Bi:Ni} = -13720 + 9.467T + .75G^{Hex}_{Bi} + .25G^{Hex}_{Ni}$

Table 2. *Considered phase and their crystal structure data*

Phase names	Common names	Struktrbericht symbol	Pearson symbol	Space group	Lattice parameters (Å)			Ref.
					a	b	c	
LIQUID	Liquid	n/a	n/a	n/a	-	-	-	-
RHOMBO_A7	(Bi)	*A*7	*hR*2	$R\bar{3}m$	4.548		11.852	[15]
FCC_A1	(Ni)	*A*1	*cF*4	$Fm\bar{3}m$	3.5243			[16] [17]
	(Pb)				4.9496			
HCP_A3	(εPb)	*A3*		$P6_3/mmc$	3.265		5.387	[18]
BI3NI	Bi_3Ni	*C*4	*oP*16	*Pnma*	8.879	4.0998	11.483	[19]
BINI	BiNi	$B8_1$	*mC*64	*F*12/*m*1	14.124	8.1621	21.429	[20]

4. Experimental results and calculations

4.1. Vertical sections

By using DTA analysis, temperatures of phase transitions for 12 studied ternary alloy samples were determined. The experimentally obtained results are summarized in Table 3. The presented phase transition temperatures were determined from the DTA results according to the literature recommendations [21, 22]. Thus, the temperatures of invariant reactions were obtained from the extrapolated onsets of the corresponding DTA peaks, whereas the temperatures of liquid and other phase transitions were evaluated from the peak maximum.

DTA heating curves of the three selected alloy samples, each belonging to one of the three studied

CC BY SA

Table 3. *Experimentally determined phase transition temperatures for the investigated alloys from the ternary Bi-Ni-Pb system*

Nominal composition (at.%)	Temperatures of phase transformation T(°C)				
	Reaction and transformation				Liquidus
	exp.[a]/calc.				exp.[a]/calc.
Vertical section x(Bi)=0.75					
$Bi_{75}Ni_5Pb_{20}$	126.2/124.9	198.5/199.9	419.6/417.9		446.7/442.5
$Bi_{75}Ni_{10}Pb_{15}$	123.4/124.9	202.7/199.9	425.2/426.8		530.1/526.5
$Bi_{75}Ni_{15}Pb_{10}$	124.7/124.9	195.8/199.9	417.8/416.1		591.8/585.4
$Bi_{75}Ni_{20}Pb_5$	123.5/124.9	198.3/199.9	409.6/416.1	450.8/451.1	631.3/626.3
Vertical section x(Pb)=0.9					
$Bi_8Ni_2Pb_{90}$	86.3/80.3	174.1/168.5	288.7/280.5		590.1/591.8
$Bi_6Ni_4Pb_{90}$	74.3/74.1	176.8/170.5			761.8/757.7
$Bi_4Ni_6Pb_{90}$	117.3/125.4	306.8/303.9			840.5/854.3
$Bi_2Ni_8Pb_{90}$	62.8/70.3	317.5/314.2			936.7/934.9
Vertical section x(Ni)=0.1					
$Bi_{70}Ni_{10}Pb_{20}$	125.8/124.9	182.1/168.3	414.8/410.5		558.3/550.3
$Bi_{50}Ni_{10}Pb_{40}$	183.1/183.5	320.9/312.8	492.3/498.1		776.5/771.2
$Bi_{30}Ni_{10}Pb_{60}$	215.1/212.4	377.5/365.7			907.1/915.7
$Bi_{10}Ni_{10}Pb_{80}$	259.7/257.8	304.8/295.7			968.5/978.1

vertical sections are presented in Fig. 2. The observed phase transition temperatures are marked on the presented heating curves (Fig. 2).

The obtained transition temperatures were compared with calculated phase diagrams. Comparison of the experimental data and the results of the calculations are presented in Figure 3.

The calculated vertical section with a constant composition of x(Bi)=0.75 mole fraction is depicted in Figure 3 a). The results of the calculation clearly show that the eutectic reaction L→Bi_3Ni+(εPb)+(Bi) occurs within the all four tested ternary alloy samples. The calculated temperature of the ternary eutectic reaction is 124.9 ºC while the experimentally determined temperatures are in the range 123.4 to 126.2 ºC. A close agreement between the calculated temperature and the experimentally determined temperatures can be observed in this case too, as in the case of the other temperatures presented in Figure 3 a).

Figure 3 b) presents the calculated vertical section with a constant composition of x(Pb)=0.9 mole fraction compared with the experimentally obtained temperatures. As can be seen from Figure 3 b), a close mutual agreement of the obtained results was obtained. Based on the conducted calculation, apart from the last temperatures which are related to the liquid phase transformation, all of the other detected temperatures are related to the other respective phase transformations.

Figure 3 c) presents the calculated vertical section with a constant composition of x(Ni)=0.1 mole fraction compared with the experimentally determined temperatures. With alloy sample $Bi_{70}Ni_{10}Pb_{20}$, it was determined that ternary eutectic reaction L→Bi_3Ni+(εPb)+(Bi) takes place at 125.8 ºC, which is close to the calculated value of 124.9 ºC. The other temperatures, detected using the same sample, correspond to different phase

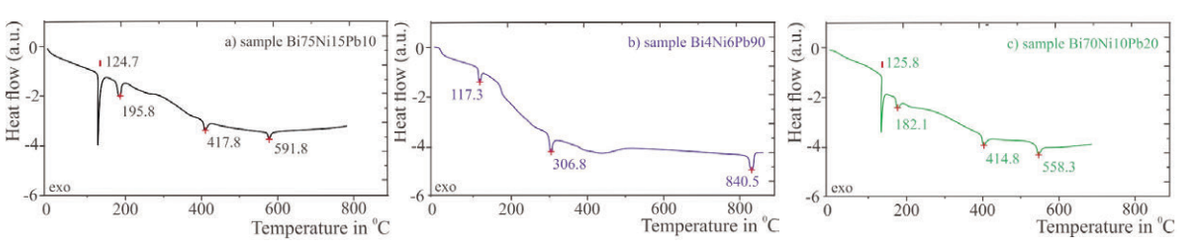

Figure 2. *DTA heating curves of the selected alloy samples, a) sample Bi75Ni15Pb10, b) sample Bi4Ni6Pb90 and c) sample Bi70Ni10Pb20*

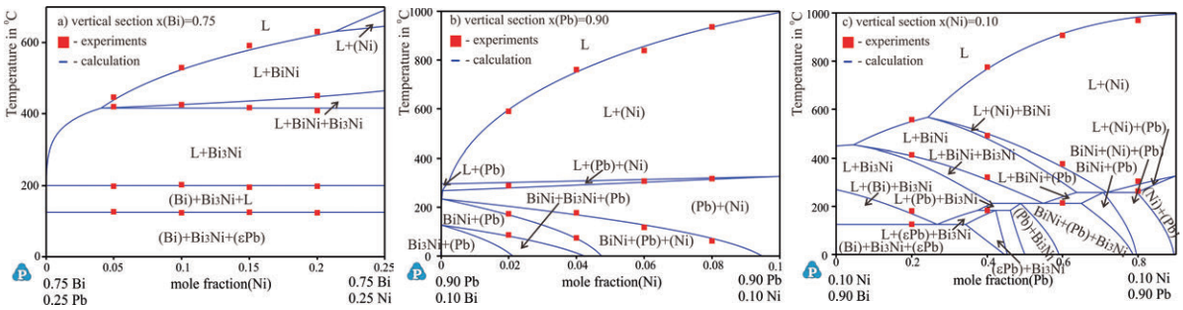

Figure 3. *Comparison between the experimental DTA results and the calculated vertical sections: a) x(Bi)=0.75, b) x(Pb)=0.9 and c) x(Ni)=0.1*

transformations, while the last one corresponds to the liquid temperature. Temperature of invariant reaction L+(Pb)→Bi_3Ni+(εPb) was determined by analysis of alloy sample $Bi_{50}Ni_{10}Pb_{40}$. The experimentally determined temperature is 183.1 ºC, while the calculated one is 183.5 ºC, which is fairly close agreement. The other detected temperatures were also found to be close to the calculated ones. The temperature of invariant reaction L+BiNi→(Pb)+Bi_3Ni was determined with alloy sample $Bi_{30}Ni_{10}Pb_{60}$. The experimentally determined temperature is 215.1 ºC, whereas the calculated one is 212.4 ºC, which is several degrees lower. The other detected temperatures are in a reasonably closer agreement with the calculated ones. With the analysis of the last alloy sample from x(Ni)=0.1, vertical section ($Bi_{10}Ni_{10}Pb_{80}$) temperature of invariant reaction L+(Ni) →BiNi+(Pb) was determined to be 259.7 ºC, while the calculated temperature is 257.8 ºC. The other two temperatures, determined using the same $Bi_{10}Ni_{10}Pb_{80}$ sample, were found to be close to the calculated values.

In general, the overall close agreement between the calculated and experimentally determined temperatures was obtained.

4.2. Isothermal section at 100 °C

The results of EDS and XRD analysis of the five alloy samples annealed at 100 ºC for eight weeks are given in Table 4. The presented data (Table 4) include overall compositions of the studied alloys, compositions of co-existing phases and their corresponding lattice parameters. The lattice parameters were determined by using full Rietveld refinement and data for comparison of the lattice parameters taken from literature [15-20].

Table 4. *Experimentally determined phase compositions in the ternary Bi-Ni-Pb system annealed at 100 °C for eight weeks*

N.	Composition of samples x(at. %)	Determined phases		Compositions of phases x(at. %)			Lattice parameters l(10^{-10}m)		
		EDS	XRD	Bi	Ni	Pb	*a*	*b*	*c*
1	15.67 Bi	BiNi	BiNi	49.89±0.4	48.13±0.2	1.98±0.7	14.1219(5)	8.1698(3)	21.4263(4)
	39.15 Ni	(Ni)	(Ni)	1.21±0.5	98.78±0.6	0.01±0.3	3.5273(4)		
	45.18 Pb	(Pb)	(Pb)	2.75±0.1	0.55±0.7	96.7±0.2	4.9528(1)		
2	20.15 Bi	BiNi	BiNi	48.65±0.4	49.52±0.5	1.83±0.5	14.1287(4)	8.1681(2)	21.4283(4)
	58.67 Ni	(Ni)	(Ni)	0.30±0.7	99.18±0.8	0.52±0.4	3.5254(4)		
	21.18 Pb	(Pb)	(Pb)	2.01±0.1	0.19±0.9	97.8±0.1	4.9508(3)		
3	40.78 Bi	BiNi	BiNi	48.69±0.2	49.63±0.2	1.68±0.2	14.1283(5)	8.1692(1)	21.4209(3)
	23.55 Ni	Bi_3Ni	Bi_3Ni	76.07±0.4	23.32±0.1	0.61±0.6	8.8764(2)	4.0976(5)	11.4887(1)
	35.67 Pb	(Pb)	(Pb)	7.51±0.5	0.31±0.4	92.18±0.7	4.9578(3)		
4	41.19 Bi	Bi_3Ni	Bi_3Ni	74.65±0.3	23.78±0.3	1.57±0.3	8.8787(4)	4.0987(3)	11.4898(5)
	4.63 Ni	(εPb)	(εPb)	33.16±0.2	0.61±0.5	66.23±0.5	3.2676(6)		5.3827(3)
	54.18 Pb								
5	68.98 Bi	Bi_3Ni	Bi_3Ni	76.76±0.4	22.89±0.7	0.35±0.7	8.8728(3)	4.0952(6)	11.4824(2)
	9.12 Ni	(εPb)	(εPb)	39.76±0.6	1.11±0.4	59.13±0.6	3.2618(1)		5.3873(1)
	21.90 Pb	(Bi)	(Bi)	98.13±0.3	0.89±0.3	0.98±0.4	4.5427(3)		11.8587(7)

CC BY SA

By analysis of the five annealed alloy samples four different phase regions were determined. In the microstructures of the samples 1 and 2 the same three phases were detected, i.e. BiNi, (Ni), and (Pb). In the sample 3 another three-phase region consisting of BiNi, Bi_3Ni, and (Pb) phases was detected. Within the sample 4, two phases Bi_3Ni and (εPb) were identified. The fourth overall phase region and the third three-phase region is Bi_3Ni+(εPb)+(Bi), which was detected in the microstructure of the alloy sample 5. Apart from the conducted EDS analysis, the additional XRD analysis was performed for identification of crystalline equilibrium phases. As can be seen from Table 4, the same phases were determined both with EDS and XRD methods. Data given in literature [15-20] was used for determination of the individual phases present in the XRD patterns of the samples 1 to 5. From Table 4, it is clear that the determined lattice parameters are in close agreement with the literature values.

Figure 4 presents two characteristic microstructures of the samples 2 and 3.

Within the microstructure of the sample 2 (Fig.4.a), three individual phases can be distinguished. The identified phases are labeled with their corresponding names. The darkest phase was identified as the solid solution (Ni), the grey phase as intermetallic compound BiNi, and the light phase as solid solution (Pb). Similarly, microstructure of the sample 3 (Fig.4.b) also represents three phases region, that consists of BiNi, Bi_3Ni, and (Pb) phases. Figure 5 presents XRD patterns of sample 3, with marked peaks of BiNi, Bi_3Ni, and (Pb) phases.

The experimental results obtained by means of EDS analysis are compared with the calculated isothermal section at 100 ºC. Figure 6 presents calculated isothermal section at 100 ^{0}C compared with the acquired experimental data.

The calculations show that the isothermal section at 100 ºC consists of eight different phase regions. Four of them are two-phases regions (Ni)+(Pb), BiNi+(Pb), Bi_3Ni+(Pb), and Bi_3Ni+(εPb), and the other four are three-phase regions (Ni)+BiNi+(Pb), BiNi+Bi_3Ni+(Pb), Bi_3Ni+(εPb)+(Pb), and Bi_3Ni+(εPb)+(Bi). Out of the eight thermodynamically predicted phase regions four were experimentally confirmed, the three three-phase regions and the one two-phase region. The (Ni)+BiNi+(Pb) three phase region was detected within the alloy samples 1 and 2, and the experimentally determined compositions of the identified phases were found to be in a close agreement with the calculated compositions.

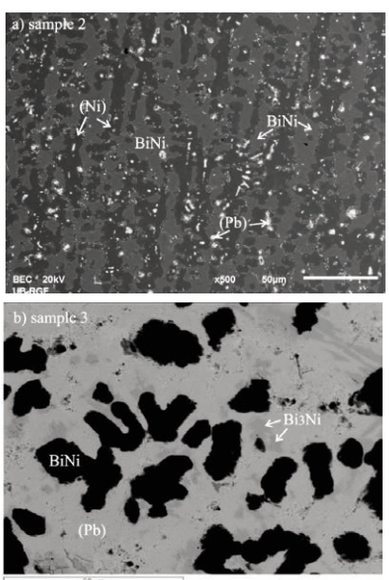

Figure 4. *SEM micrographs of the selected alloy samples annealed at 100 °C for eight weeks: a) sample 2 and b) sample 3*

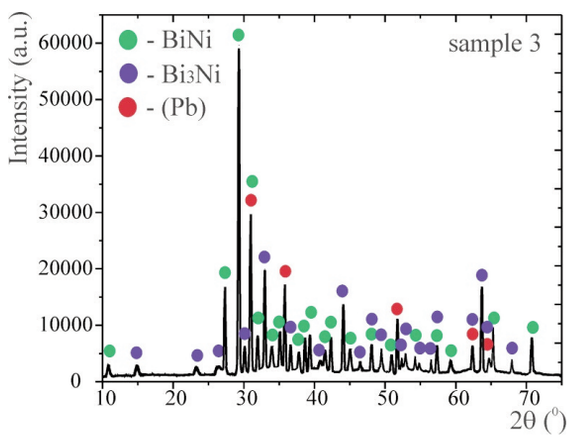

Figure 5. *XRD pattern for the alloy sample 3*

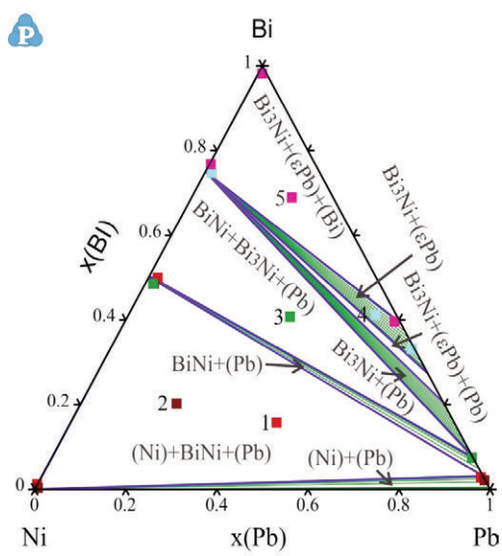

Figure 6. *The calculated isothermal section at 100 °C compared with the experimental data*

Existence of the BiNi+Bi_3Ni+(Pb) three-phase region was confirmed within the sample 3. The experimentally determined compositions of these three phases are marked with green squares in Fig. 6, and it can be seen that in this instance also close agreement between the experimental and the calculated compositions was obtained. Within the microstructure of the sample 4 the two-phase Bi_3Ni+(εPb) region was observed while the three-phase region Bi_3Ni+(εPb)+(Bi) was detected in the sample 5. On the whole, a general close agreement of the calculated and the experimentally determined compositions of the identified phases can be noticed in Fig. 6.

4.3. Isothermal section at 300 °C

In the same manner as in the previous case, the six alloy samples were annealed at 300 °C for five weeks. The annealed samples were subsequently used for investigation of the existing phase regions at the selected temperature. The obtained experimental results of EDS and XRD analysis that include overall alloy compositions, compositions of co-existing phases, and their lattice parameters are summarized in Table 5. For determination of the lattice parameters full Rietveld refinement was employed while the data used for comparison of the lattice parameters were taken from literature [16, 19-20].

The obtained experimental results indicate existence of five different phase regions. Two phases were identified in the sample 1 at equilibrium, one of them is the Ni-rich phase and the second one is the Pb-rich phase with some amount of Bi. Within the samples 2 and 3 three phases were detected, the first Ni-rich phase, the second phase with a similar ratio of Bi and Ni and negligible amount of Pb, and the third Pb-rich phase with some amount of Bi and negligible amount of Ni. The obtained XRD patterns of the samples 2 and 3 were compared with patterns of (Ni) solid solution [16] and intermetallic compound BiNi [20]. After the peak identification, it was confirmed that the observed phases in the studied samples are in fact (Ni) and BiNi, however, no other phase was detected. So the third phase identified using EDS analysis is most probably Liquid phase. Two different two-phase regions were observed within the microstructures of the samples 4 and 6, which both contain Liquid phase and an intermetallic compound. The BiNi intermetallic compound was identified in the sample 4 and the Bi_3Ni in the sample 6. The microstructure of the sample 5 was found to consist of three phases: BiNi, Bi_3Ni, and Liquid phase. Two characteristic microstructures of the alloy samples 3 and 4 are presented in Figure 7.

Table 5. *Experimentally determined phase compositions in the ternary Bi-Ni-Pb system annealed at 300 °C for five weeks*

N.	Composition of samples x(at. %)	Determined phases		Compositions of phases x(at. %)			Lattice parameters l(10^{-10}m)		
		EDS	XRD	Bi	Ni	Pb	*a*	*b*	*c*
1	12.89 Bi	(Ni)		0.56±0.5	99.03±0.2	0.41±0.2	3.5252(3)		
	27.13 Ni	L	(Ni)	18.05±0.8	0.31±0.4	81.54±0.6			
	59.98 Pb								
2	20.18 Bi	BiNi	BiNi	49.45±0.3	49.18±0.6	1.37±0.6	14.1238(4)	8.1652(5)	21.4248(2)
	64.06 Ni	(Ni)	(Ni)	0.92±0.2	98.87±0.6	0.21±0.7	3.5273(1)		
	15.76 Pb	L		23.89±0.5	1.24±0.2	74.87±0.9			
3	32.89 Bi	BiNi	BiNi	48.08±0.4	50.13±0.7	1.79±0.2	14.1265(2)	8.1698(1)	21.4228(3)
	40.10 Ni	(Ni)	(Ni)	0.76±0.3	98.56±0.5	0.68±0.1	3.5279(3)		
	27.01 Pb	L		24.18±0.2	0.09±0.2	75.73±0.4			
4	42.18 Bi	BiNi		51.27±0.7	48.54±0.2	0.19±0.8	14.1219(1)	8.1676(4)	21.4252(1)
	18.95 Ni	L	BiNi	32.18±0.3	2.68±0.6	65.14±0.9			
	38.87 Pb								
5	59.43 Bi	Bi_3Ni	Bi_3Ni	74.12±0.2	24.83±0.7	1.05±0.3	8.8772(8)	4.0983(2)	11.4827(8)
	28.92 Ni	BiNi	BiNi	49.02±0.1	49.15±0.5	1.83±0.2	14.1246(4)	8.1627(5)	21.4238(1)
	11.65 Pb	L		48.63±0.5	0.39±0.3	50.98±0.6			
6	72.18 Bi	Bi_3Ni		76.08±0.8	23.76±0.8	0.16±0.7	8.8763(3)	4.0928(5)	11.4859(4)
	9.37 Ni	L	Bi_3Ni	71.54±0.6	0.27±0.9	28.19±0.5			
	18.45 Pb								

CC BY SA

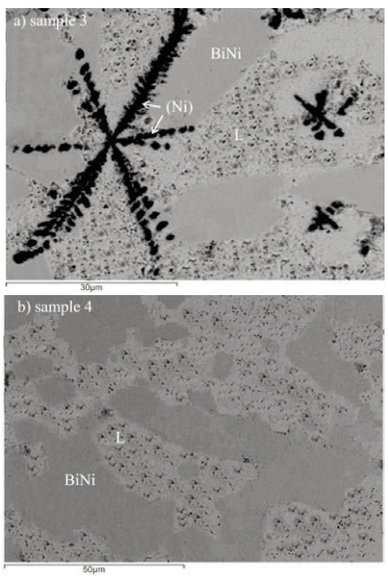

Figure 7. *SEM micrographs of the selected alloy samples annealed at 300 °C for five weeks: a) sample 3 and b) sample 4*

Fig. 7 a) presents microstructure of the sample 3, in which three phases are visible. The identified phases are marked with their corresponding names. The darkest phase in Fig. 7 a) is a (Ni) solid solution, the grey phase is a binary intermetallic compound BiNi, and the light phase is a Liquid, L phase. Within the microstructure of the sample 4, presented in Figure 7 b), two phases in equilibrium can be observed, the grey phase which is a BiNi intermetallic compound and the light phase which represents a Liquid, L phase.

Figure 8 presents XRD patterns of sample 6, with marked peaks of Bi_3Ni phase.

The experimentally obtained EDS results for the samples annealed at 300 ºC were compared with the calculated isothermal section at 300 ºC. Figure 9 presents the calculated isothermal section at 300 ºC compared with the obtained experimental data.

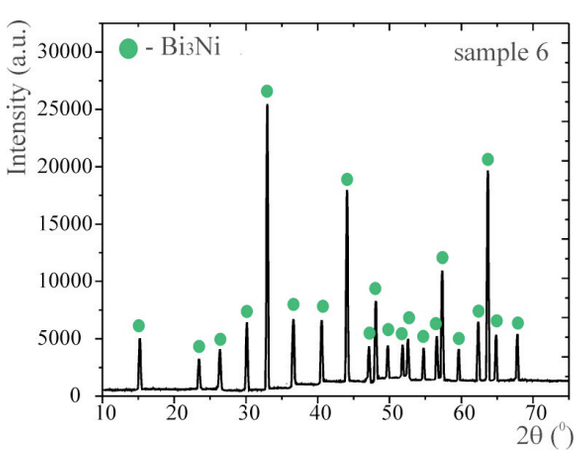

Figure 8. *XRD pattern for the alloy sample 6*

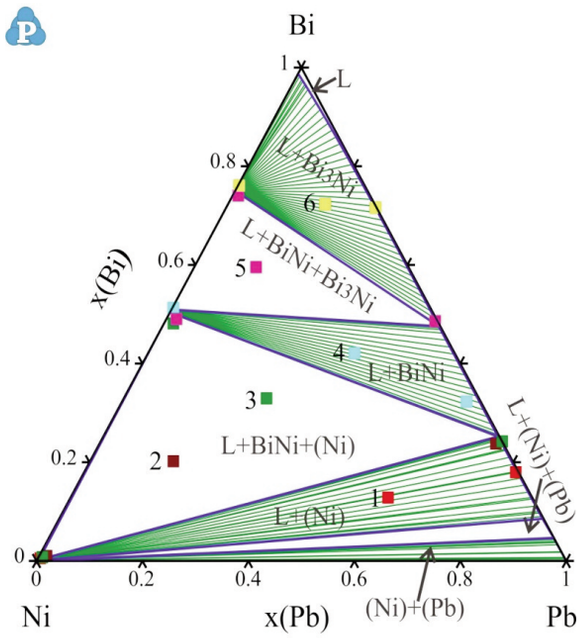

Figure 9. *The calculated isothermal section at 300 ºC compared with the experimental data*

The calculated isothermal section at 300 ºC was found to consist of eight different phase regions. One is single-phase region where Liquid, L phase exist, four are two-phase regions (Ni)+(Pb), L+(Ni), L+BiNi, and L+Bi_3Ni, and remaining three are three-phase regions L+(Ni)+(Pb), L+BiNi+(Ni), and L+BiNi+Bi_3Ni. Five out of the eight phase regions predicted by thermodynamic calculations were experimentally detected, the three two-phase regions and the two three-phase regions. The existence of the two-phase regions L+(Ni), L+BiNi, and L+Bi_3Ni was confirmed within the alloy samples 1, 4 and 6, respectively. Within the samples 2 and 3, presence of the three-phase region L+BiNi+(Ni) was confirmed, and within the sample 5 presence of the another three-phase region L+BiNi+Bi_3Ni was confirmed. The determined compositions of the studied alloy samples and each of the identified phases are marked in Figure 9 (the same color of squares was used for marking of the sample compositions and compositions of the associated phases). From Fig. 9 it can be seen that the experimentally determined phase compositions support the results of thermodynamic calculations rather well.

Considering that the general close agreement was achieved between the experimental results (DTA, EDS, and XRD analyzes) and the calculated phase diagrams (vertical section and isothermal sections), it was concluded that it was not necessary to add new thermodynamic parameters for description of the ternary Bi-Ni-Pb system. The used thermodynamic data sets for the constitutive binary systems [9-13] can

CC BY SA

represent the phase diagram of the ternary Bi-Ni-Pb system quite well.

5. Prediction of liquidus projection

Considering that in the case of calculations of the conducted isothermal sections the close agreement between the calculated and the experimental results was obtained, the same thermodynamic data set was used for further calculations related to the phase diagram of the ternary Bi-Ni-Pb system.

Figure 10 presents the predicted liquidus projection of the ternary Bi-Ni-Pb system with an insert showing the enlarged Pb-rich region (for better insight into positions of invariant reactions).

Table 6 presents the predicted invariant reactions involving the liquid phase of the Bi-Ni-Pb ternary system.

According to the obtained results of the thermodynamic calculations, four invariant reactions appear in the ternary Bi-Ni-Pb system and all of them are experimentally detected by DTA. $L \rightarrow Bi_3Ni+(\varepsilon Pb)+(Bi)$ reaction was detected in the five studied alloy samples and the temperature of this reaction was determined to be in the range 123.4 to 126.2 ºC. Invariant reaction $L+(Pb) \rightarrow Bi_3Ni+(\varepsilon Pb)$ was detected in the $Bi_{50}Ni_{10}Pb_{40}$ alloy sample at the temperature of 183.1 ºC. Reaction $L+BiNi \rightarrow (Pb)+Bi_3Ni$ was observed to occur in the sample $Bi_{30}Ni_{10}Pb_{60}$ at 215.1 ºC while $L+(Ni) \rightarrow BiNi+(Pb)$ reaction was observed in alloy sample $Bi_{10}Ni_{10}Pb_{80}$ at 259.7 ºC. All of the experimentally determined reaction temperatures were found to be close to the thermodynamically calculated values.

6. Conclusions

Ternary Bi-Ni-Pb system has been experimentally examined by DTA, EDS and XRD techniques. The results of DTA were used for detection of phase transition temperatures for 12 investigated ternary alloy samples. The collected experimental results were compared with calculated vertical sections and a close agreement between the results was observed.

The alloy samples annealed at 100 and at 300 °C were analyzed using EDS and XRD. The conducted EDS analysis has not revealed any new compound or solubility of the third element into the binary compounds or large solubility of other two elements

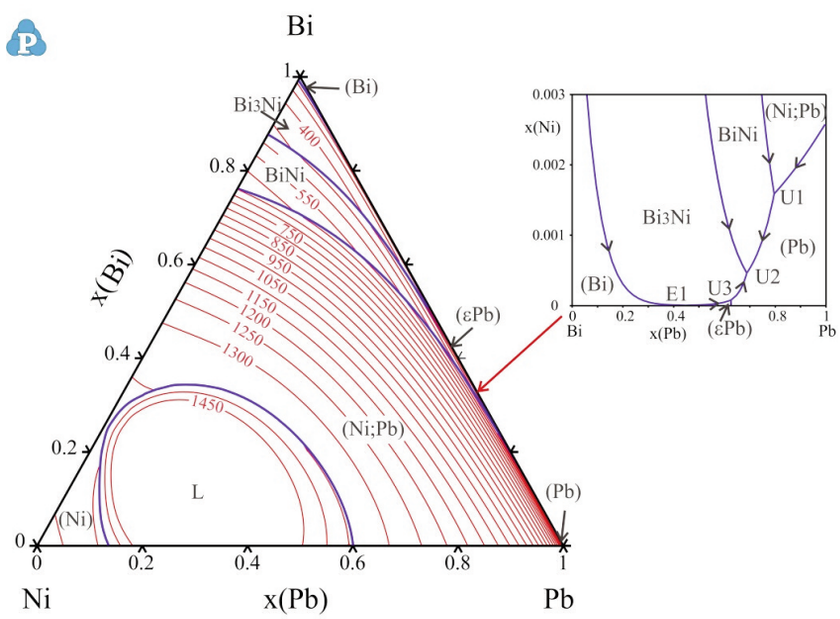

Figure 10. *Predicted liquidus projection of the ternary Bi-Ni-Pb system*

Table 6. *Predicted invariant reactions involving the liquid phase of the Bi-Ni-Pb ternary system*

Temperature in °C	Invariant reaction	Type	at. %(Bi)	at. %(Ni)	at. %(Pb)
257.8	$L+(Ni) \rightarrow BiNi+(Pb)$	U1	20.3	0.15	79.55
212.4	$L+BiNi \rightarrow (Pb)+Bi_3Ni$	U2	31.2	0.05	68.75
183.5	$L+(Pb) \rightarrow Bi_3Ni+(\varepsilon Pb)$	U3	37.47	0.01	62.52
124.9	$L \rightarrow Bi_3Ni+(\varepsilon Pb)+(Bi)$	E1	55.35	0.01	44.64

CC BY SA

into solid solutions. A close agreement between the experimental results and the calculated isothermal sections was obtained in this case as well.

Thermodynamic calculations of the studied vertical and isothermal sections were carried out using parameters for the binary sub-systems. The subsequent comparison of the calculated and the gathered experimental results has shown that the experimental data support the results of the calculations quite well. This led to a conclusion that it is not necessary to introduce ternary interaction parameters for the description of the phase diagram of the ternary Bi-Ni-Pb system.

Acknowledgements

This work has been supported by the Ministry of Education, Science and Technological Development of the Republic of Serbia (Grant No. OI172037).

References

[1] N. Saunders, A. P. Miodownik: CALPHAD (Calculation of Phase Diagrams): a comprehensive guide, (R.W. Cahn), Pergamon Materials Series, vol. 1, Elsevier Science Ltd., London, 1998.

[2] B. Sundman, J. Min. Metall. Sect. B-Metall., 53(3)B (2017) 173-177.

[3] W. Cao, S.-L. Chen, F. Zhang, K. Wu, Y. Yang, Y.A. Chang, R. Schmid-Fetzer, W.A.Oates, Calphad, 33(2) (2009) 328–342.

[4] B. Sundman, B. Jansson, J. O. Andersson, Calphad, 9 (1985) 153–190.

[5] B. Sundman, U. R. Kattner, M. Palumbo, S. Fries, Integr. Mater. Manuf. Innov., 4(1) (2015) 1-15.

[6] G.P. Vassilev, K.I. Lilova, J.-C. Gachon, J. Min. Metall. Sect. B-Metall., 43B(2) (2007) 141-150.

[7] V. D. Gandova, J. Min. Metall. Sect. B-Metall., B52(1) (2016) 113-118.

[8] M. Premovic, D. Minic, D. Manasijevic, V. Cosovic, D. Živkovic, Irma Derviševic, Thermochim. Acta., 609 (2015) 61–74.

[9] G. P. Vassilev, J. Romanowska, G. Wnuk, Intern. J. Mater. Res. (former Z. Metallkunde), 98(6) (2007) 468-475.

[10] G. Vassilev, V. Gandova, P. Docheva, Cryst. Res. Technol., 44(1) (2008) 1-6.

[11] A. Dinsdale, A. Watson, A. Kroupa, J. Vrestal, A. Zemanova, J. Vizdal: Atlas of Phase Diagrams for the Lead-Free Soldering, COST 531 (Lead-free Soders), Vol. 1, © COST office, 2008.

[12] D. Boa, I. Ansara, Thermochim.Acta., 314(1) (1998) 79-86.

[13] C. P. Wang, X. J. Liu, I. Ohnuma , R. Kainuma, K. Ihida, Calphad., 24(2) (2000) 149-167.

[14] International Centre for Diffraction Data, ICDD, PDF-2 2013, 12 Campus Blvd., Newtown Square, PA 19073-3273 U.S.A.

[15] W. P. Davey, Phys. Rev., 25 (1925) 753-761.

[16] E. A. Owen, E. L. Yates, Philos. Mag., 7(21) (1936) 809-819.

[17] E. A. Owen, E. L. Yates, Philos. Mag., 7(15) (1933) 472-488.

[18] T. Takahashi, H. K. Mao, W. A. Bassett, Science, 165 (1969) 1352-1353.

[19] E. L. Martinez Pineiro, B. L. Ruiz Herrera, R. Escudero, L. Bucio, Solid State Commun., 151 (2011) 425-429.

[20] M. Ruck, Z. Anorg. Allg. Chem., 625 (1999) 2050-2054.

[21] J. C. Zhao, Methods for Phase Diagram Determination, Elsevier, 2007.

[22] P. Fima, A. Gazda, J. Therm. Anal. Calorim., 112 (2013) 731–737.

EKSPERIMENTALNO ISPITIVANJE I TERMODINAMIČKA ANALIZA Bi-Ni-Pb FAZNOG DIJAGRAMA

D. Minić [a,*], M. Premović [a], N. Tošković [b], D. Manasijević [c], V. Ćosović [d], M. Janaćković [a], M. Tomović [a]

[a] Univerzitet u Prištini, Fakultet tehničkih nauka, Kosovska Mitrovica, Srbija
[b] Univerzitet u Istočnom Sarajevu, Tehnološki fakultet Zvornik, Bosna i Hercegovina
[c] Univerzitet u Beogradu, Tehnički fakultet u Boru, Bor, Srbija
[d] Univerzitet u Beogradu, Institut za hemiju, tehnologiju i metalurgiju, Beograd, Srbija

Apstrakt

U ovom radu je predstavljeno eksperimentalno ispitivanje faznog dijagrama Bi-Ni-Pb ternarnog sistema uz pomoć diferencijalne termijske analize (DTA), skenirajućeg elektronskog mikroskopa (SEM) sa energijsko disperzivno spektrometrijom (EDS) i rentgenskom difrakcijom praha (XRD). Ispitivane ternarne legure su izabrane iz tri vertikalna preseka (x(Bi)=0.75, x(Ni)=0.1 i x(Pb)=0.9), i dva izotermalna preseka na 100 i 300°C. Rezultati eksperimenta su upoređeni sa termodinamički ekstrapolisanim faznim dijagramom Bi-Ni-Pb ternarnog sistema na osnovu termodinamičkih parametara sastavnih binarnih sistema koji su dostupni u literaturi. Utvrđeno je dobro slaganje između eksperimentalnih rezultata i proračunatog faznog dijagrama.

Ključne reči: *Bi–Ni-Pb sistem; Vertikalni preseci (x(Bi)=0.75, x(Ni)=0.1 i x(Pb)=0.9); Izoterermalni preseci na 100 i 300°C; Termijska analiza; Termodinamičko predviđanje.*

CC BY SA